Chemistry Europe
European Chemical Societies Publishing

WILEY VCH

# Excellence in Chemistry Research


## Announcing our new flagship journal

- Gold Open Access
- Publishing charges waived
- Preprints welcome
- Edited by active scientists

## Meet the Editors of *ChemistryEurope*

**Luisa De Cola**
Università degli Studi di Milano Statale, Italy

**Ive Hermans**
University of Wisconsin-Madison, USA

**Ken Tanaka**
Tokyo Institute of Technology, Japan

ChemistrySelect

Research Article
doi.org/10.1002/slct.202303040

Chemistry Europe
European Chemical Societies Publishing

www.chemistryselect.org

# 2D Coordination Polymers Based on Isoquinoline-5-Carboxylate and Cu(II)

Mattia Maffeis,[a] Lorenza Draghi,[a] and Massimo Cametti*[a]

By combining isoquinoline-5-carboxilic acid with Cu(II) ions under several different conditions, we were able to obtain novel metallorganic materials, among which two 2D coordination polymers, CP **1** and CP **2** which were also characterized by SC-XRD. Ratio of solvents (EtOH:DMF) in the mixture employed during their synthesis has a marked effect in selecting the formation of one species or the other, which basically differ in the coordination at the Cu(II) center due to $k^1/k^2$ denticity of the carboxylate ligands.

## Introduction

Material chemistry is nowadays benefiting from the contribution of an increasing number of studies on coordination polymers (CPs), a class of compounds formed by the combination of metal ions or clusters with organic ligands. Given their high crystallinity, modular design, uncomplicated synthetic procedures and unique physico-chemical properties, they are believed to possess the potential to revolutionize many different applications.[1]

Although the multitude of different metal-ligand combinations is anything but limited, the use of heteroditopic ligands (*i.e.*, ligands with two different metal binding sites), extends even further the CPs chemical space in terms of possible metal – ligand interaction geometries, eventually leading to novel topologies, architectures and resulting properties.[2]

Neutral pyridinic groups and negatively charged carboxylates are the most common metal coordinating units,[3] hence it is quite unsurprising that nicotinic and isonicotinic acids (Scheme 1a), combining both moieties onto a single aromatic ring, have been quite successful in the formation of a variety of CPs in combination with many different d-block metal ions. Intriguing magnetic properties, SHG, heterobimetallic systems and topologies have been obtained, also in combination with additional co-ligands.[4] As far as adsorption applications are concerned, J. Y. Lu *et al.* described the first Cu(II) isonicotinic acid 3D MOF ($Cu(INA)_2$) (INA = isonicotinic acid carboxylate) capable to adsorb different alcohols, and also selectively EtOH from mixtures, in a SC-to-SC fashion.[5] More recently, $Cu(INA)_2$ has also been studied as ethylene adsorbent.[6]

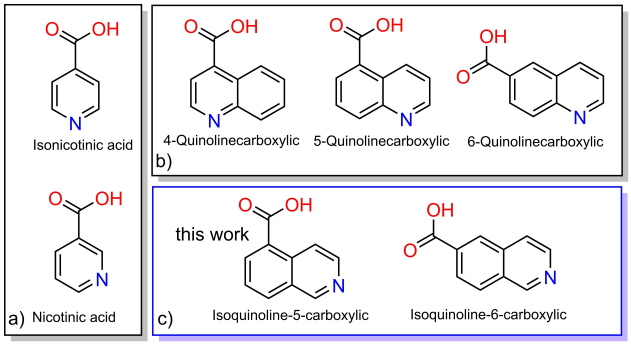


**Scheme 1.** Molecular formulae of heteroditopic a) nicotinic and isonicotinic acids, b) 4-, 5- and 6-quinoline carboxylic acids and c) isoquinoline-5-carboxylic and isoquinoline-6-carboxylic acids.

In order to modulate the CPs properties, the size of the ligand can be varied while keeping the typology of the main donor units, for example by extending the aromatic surface by one or more rings, a classic endeavour in reticular chemistry.[7] Although fewer in number, reports about CPs made with 4-, 5- and 6-quinolinecarboxylic acids (Scheme 1b) are available and they describe the formation of porous and non-porous CPs of various dimensionalities.[6,8] In particular, 5-quinolinecarboxylic acid forms 3D MOFs with Cu(II) which were demonstrated to possess a significant affinity for $O_2$.[8c]

To the best of our knowledge, instead, isoquinoline-5- and isoquinoline-6-carboxilic acids (Scheme 1c) have been never tested with the purpose of CP formation. There is only one structural report on the former ligand in the form of a phosphate salt.[9]

Here, we explored the formation of CPs made with isoquinoline-5-carboxylic acid and Cu(II) ions by using different solvent systems (EtOH/DMF mixtures) and synthetic routes. We found out that, at r.t., two 2D CPs, **1** and **2** can be assembled, and depending on the ratio of EtOH and DMF in the mixture used in their synthesis, the exclusive formation of one CP or the other can be attained, showing the occurrence of a remarkable solvent templating effect.[10] We were also able to characterize the two materials *via* SC-XRD to reach their full structural description. Conversely, under refluxing conditions, and regard-

[a] *M. Maffeis, Prof. L. Draghi, Prof. M. Cametti*
*Department of Chemistry, Materials and Chemical Engineering "Giulio Natta", Politecnico di Milano, Via Luigi Mancinelli 7, 20131 Milano, Italy*
*E-mail: massimo.cametti@polimi.it*

*Supporting information for this article is available on the WWW under https://doi.org/10.1002/slct.202303040*

less of the DMF:EtOH solvent ratio employed, a third material, **3**, different from the previous two, was obtained. While CP **2** and **3** are stable for several weeks under ambient conditions, CP **1** transforms into a different microcrystalline phase CP **1'** after a few days.

## Results and Discussion

Synthesis of microcrystalline CPs was initially performed by varying the ratio of a DMF:EtOH mixture at room temperature. It can be easily shown that in cases when there is either a predominance of DMF, or of EtOH, a single phase, but one different from the other, is present. Best results, in terms of crystallinity and yields, were obtained with a solvent ratio of 3:1 (and 1:3) (Figure S1, ESI). On the contrary, by using more balanced ratios, a mixture of the two phases was obtained (Figure S2 ESI). Based on these data, we also carried out slow crystallizations experiments in order to obtain SCs and have a full structural characterization of the two crystalline materials. Good quality SCs of CPs **1** and **2** were obtained by slow evaporation of a 3:1 (or 1:3) DMF:EtOH mixture of isoquinoline-5-carboxylic acid and $Cu(OAc)_2$ in a 2:1 ratio and then characterized by SC-XRD. CP **1** consists in violet polyhedric crystals with visible irregular hexagonal shaped faces (Figure 2a). The Cu(II) centres are in a distorted octahedral environment enforced by two $k^2$ carboxylate donors on the equatorial plane and two quinoline Ns in the apical positions (Figure 2b). Overall, this generates a 2D topology, with each layer offset with respect to the next (Figure S3, ESI), but still forming square shaped channels filled with ordered DMF molecules (Figure 2c), weakly HB-interacting with quinoline CHs ($CH_{arom}\cdots O{=}C_{DMF}$ = 2.483 Å). Virtual removal of the included solvent frees ca. 42.1% of the total unit cell volume (Figure S3 ESI).[11] Inter-layer interactions are mainly of the $CH_{arom}\cdots O_{carboxylate}$ type (2.411 Å).

CP **2** is instead made of large right-rhombic prismatic blocks of blue colour (Figure 3a). As previously, the Cu(II) ions maintain an octahedral coordination geometry with the two quinoline nitrogens in the apical position. However, in this case, the two carboxylates behave differently, with only one of the two chelating the metal center in a $k^2$ fashion, and the other acting as monodentate (Figure 3b). Hence, the fourth equatorial site is taken by a coordinated DMF molecule (slightly distorted over two positions, Cu(II)···O=C = 2.437 Å). Overall, the CP has a 2D topology, with multiple hydrogen-bonded layers ($CH_{arom}\cdots O_{carboxylate}$ HBs in the 2.486–2.651 Å range) which align one on the top of the others (Figure 3c) leaving some voids (making ca. 13% of the total unit cell volume, see Figure S3 in ESI)[11] which are filled with disordered EtOH molecules. Structural dissimilarity between CP **1** and **2** is mainly related to

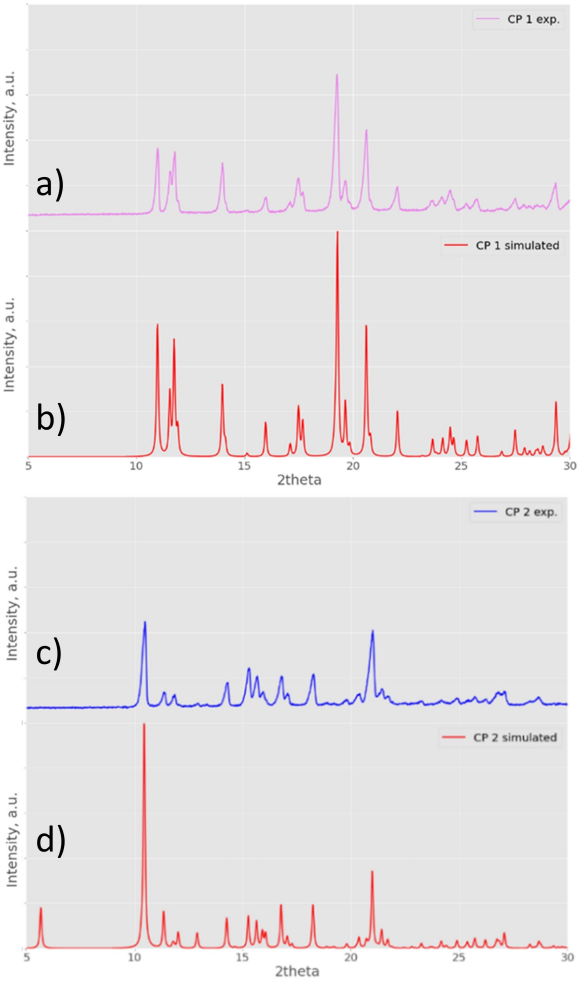


**Figure 1.** P-XRD pattern of microcrystalline CP **1** (a) compared with the simulated data derived from SC-XRD analysis on single crystals (b); P-XRD pattern of CP **2** (c) compared with the simulated data derived from SC-XRD analysis on single crystals (d).

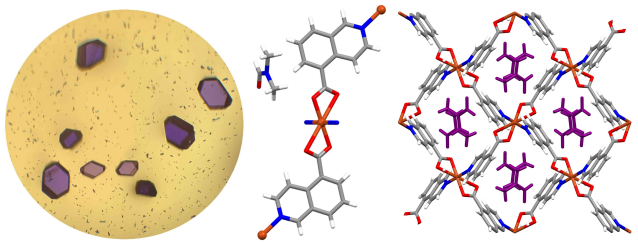

**Figure 2.** a) View of the violet crystals of CP **1** by optical microscope; b) view of the coordination sphere of the Cu(II) ion and relative position of the ligand, and included solvent; c) view of the packing in CP **1** along the *a*-axis, highlighting the trapped DMF molecules in purple colour. Colour code: N = blue, C = grey, O = red, H = white, $Cu^{II}$ = orange.

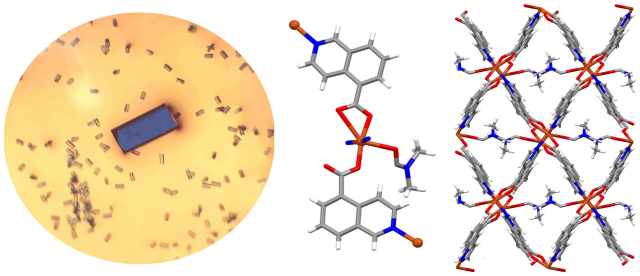

**Figure 3.** a) View of the blu crystals of CP **2** by optical microscope; b) coordination sphere of the Cu(II) ion and relative position of the ligand, and coordinated solvent; c) view of the packing in CP **2** along the *a*-axis. Colour code: N = blue, C = grey, O = red, H = white, $Cu^{II}$ = orange.

the $k^1/k^2$ nature of the coordination by carboxylates to the Cu(II), the derived role of the DMF within the structure and the different offset of adjacent 2D layers. All this results in a marked tilting of the aromatic rings with respect to the equatorial coordination plane for CP **2** (of ca. 75 deg., see Figure S4 in ESI).

The simulated P-XRD patterns of CP **1** and CP **2** derived from SC-XRD data were compared to the respective experimental diffractograms in Figure 1 (left for CP **1** and right for CP **2**), thus determining the structural characteristics and identifying of the two abovementioned microcrystalline powders. The difference between the two phases is mainly attributed to the different role of the solvent molecules DMF and EtOH in the two CPs. As said, in CP **1**, DMF molecules are located into linear channels which they thus fill, while in CP **2**, DMF solvent is coordinated to the metal center and additional EtOH are also present within not interconnected lattice pockets. TGA characterization confirms the presence of one (DMF) or two different solvents (DMF and EtOH) within the 2D structures (Figure S5–S6, ESI). Interestingly, since both materials are obtained under the same r.t. conditions, we can relate the different outcome solely to the solvent system which evidently can determine whether DMF is coordinated or not.

In order to better understand the underlying process of formation of the two materials, we have also performed the synthesis in pure EtOH and in pure DMF (neither solvents were anhydrous, so 0.1–0.5% water can be expected). In this latter case, CP **1** was formed, while in pure EtOH a different phase, at the moment unknown was obtained (Figure 8 ESI). Also, we monitored the effect of time. The CP synthesis in 3:1 DMF:EtOH kept under stirring for prolonged time (7–21 days) resulted in a mixtures of the two phases. This indicates that CP **2** which indeed forms over longer period of time at the expense of CP **1** is thermodynamically more stable, and that the presence of increasing quantities of EtOH accelerates its formation. Given that in pure DMF CP **1** is formed, evidently the role of EtOH is to either facilitate the coordination of DMF to the metal center (that eventually will occur as CP **1** transforms in CP **2** over longer reaction times), or to compete with the Cu(II) ions for the carboxylate moiety, or both. In CP **2**, the uncoordinated carboxylate oxygen is directly facing the pockets which entraps the disordered ethanol molecules so to also suggest a possible structure directing templating effect of EtOH. Notably, while CP **2** is stable in open air for at least 2 weeks, CP **1** transforms over time (3–7 days) losing its characteristic violet colour generating a new phase named CP **1'** (Figure 4, top). Finally, when reaction between isoquinoline-5-carboxylic acid and Cu(II) salts ($NO_3$, $BF_4$, etc..) was carried out under refluxing conditions, regardless of the DMF:EtOH solvent ratio used, a third phase of green colour, named 3, was observed (Figure 4, bottom). We failed in reproducing this material as SCs, thus its structural features remain at the moment unknown. TGA analysis however indicates the absence of solvents within its lattice (Figure S7 ESI).

As a side note, crystallization attempts with acetate or nitrate Co(II) salts with DMF/EtOH solvent mixture ratios from 1:5 to 5:1 afforded, in all cases, light orange crystals which, analysed by SC-XRD, were revealed to be 1:2 metal:ligand

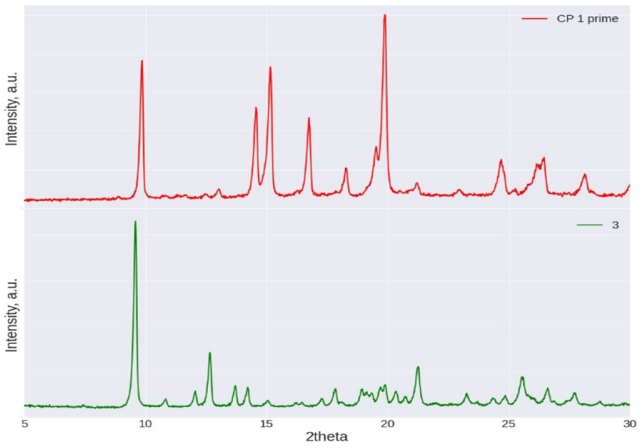


**Figure 4.** P-XRD data for CP **1'** (top) and **3** (bottom).

molecular complexes, as shown in Figure 5a. In this case, the octahedral Co(II) is coordinated by four water molecules on its equatorial plane and by the two isoquinoline ligands, via the N atom. Thus, the coordinative polymerization is stopped and the carboxylate – metal interaction occurs in the metal second sphere coordination,[12] as shown in Figure 5b, with strong HB CO*O*···$H_2O$–Co = 2.698, 2.759 Å). This type of complexes is slightly more common for Co(II) ions than for Cu(II) (approx. 200 entries in the CSD *vs. ca.* 80 for Cu(II)). This molecular complex phase can be obtained in the form of microcrystalline powders also by keeping at 70 °C a 1:1 mixture of $Co(NO_3)_2$ and the ligand in DMF:EtOH 1:1 for 24 h, as demonstrated by comparing the P-XRD pattern of the powder resulted from the abovementioned process with the simulated pattern from SC data (Figure 5c).

ATR-FT-IR analysis of all CP samples and **3** is shown in Figure 6. For CP **1**, bands at ca. 1670 $cm^{-1}$ and 1095 $cm^{-1}$ (corresponding to C=O stretching and N–$CH_3$ rocking), and the band at ca. 1395 $cm^{-1}$ (multiple contribution among which $CH_3$ deformation and C–N stretching) are tentatively assigned to the DMF molecules within its channels.[13] Indeed, these bands are not present in CP **1'**, nor in **3**, devoid of the solvent. Noticeable differences between CP **1** and CP **2** spectra are present and

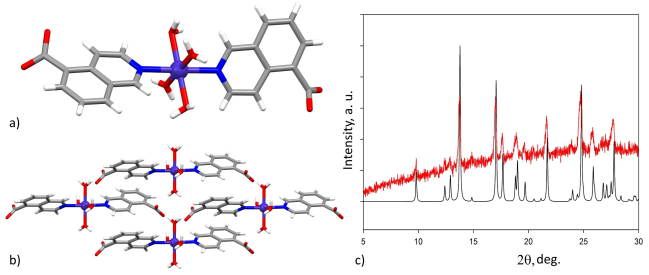


**Figure 5.** View of the molecular complex [$Co^{II}$(isoquinoline-5-carboxylate)$_2$($H_2O$)$_4$] (top) and its HB directed packing (bottom). Colour code: N = blue, C = grey, O = red, H = white, $Co^{II}$ = purple; c) P-XRD pattern of microcrystalline powder obtained by reacting Co(II) with isoquinoline-5-carboxylic acid compared with the corresponding simulated data from SC-XRD.

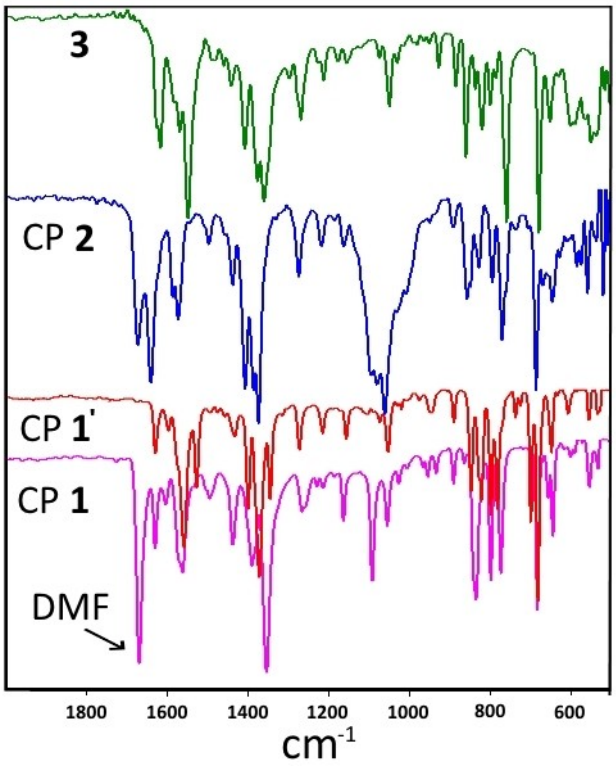


**Figure 6.** From bottom to top, ATR-FTIR spectra of CP **1** (purple), CP **1'** (red), CP **2** (blu) and **3** (green).

they can be attributed to the different metal-ligand configuration which the carboxylates groups adopt in the two structures. Powders of CP **1**, CP **2** and **3** were subjected to thermal treatment (100 °C) under vacuum. As shown by the P-XRD patterns obtained (Figure 7), it appears that both CP **1** and CP **2** lose crystallinity, while **3** is not affected. We tentatively attribute this different behaviour to the fact that **3** possesses no inclusion solvent and, being formed under refluxing conditions, it has probably achieved a more stable and robust framework architecture. The materials were also tested for porosity by BET analysis. As hinted by the loss of crystallinity observed under reduced pressure conditions both CP **1** and **2** show very little available surface area (in the 5–15 $m^2/g$) (Figures S9 and S10 ESI), while **3** shown no $N_2$ adsorption whatsoever. Both CP **1** and CP **2**, their desolvated phases, and **3** were exposed within a closed chamber to vapours of Chlorobenzene (ClBz), Nitrobenzene (NB) and toluene for 3–7 days. CP **2** and **3** did not transform, while CP **1** changed into CP **1'**, being thus unaffected by the presence of the abovementioned aromatic solvents in the reaction chamber. Dipping SCs of CP **1** into ClBz and NB destroys the crystals in less than 30 minutes, while CP **2** is unaffected by the mentioned treatment. Finally, $CO_2$ adsorption was tested for CP **1** by TGA, but a merely 0.065% increase in weight after 1 h exposure in a 100% atmosphere of $CO_2$ was observed (Figure S11, ESI).

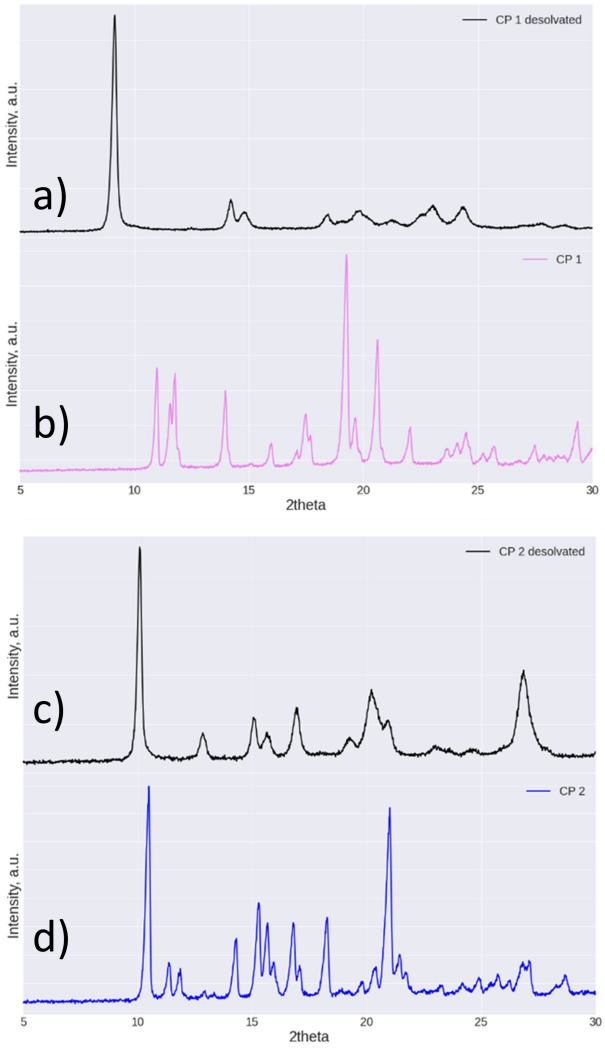


**Figure 7.** P-XRD data for a) CP **1** after desolvation compared to b) the corresponding starting material, and c) CP **2** after desolvation compared to d) the corresponding starting material.

## Experimental Details

All reagents were purchased from Fluorochem Ltd. and used without further purification. SC X-ray structures were collected with Bruker Kappa Apex II (Mo–Kα radiation) and with a Rigaku XtaLAB Synergy-i. P-XRD patterns were collected with a Bruker D2-Phaser (Cu radiation λ = 1.54184 Å) with Bragg-Brentano geometry; TGA analyses were performed with SDT Q600 operating in the 30–400 °C range; ATR-FT-IR analyses were carried out with a VARIAN 640-IR.

*CP synthesis as microcrystalline powders*: In a 50 mL flask, 200 mg of isoquinoline-5-carboxylic acid, 200 mg of $Cu(BF_4)_2$ hexahydrate and 25 mg ZnO are added; then, a mixture of DMF and Ethanol (25 mL) is added and the mixture is kept under stirring (at r.t.). As described in the text, the solvent ratio is crucial for the obtainment of the desired product: for example, a 3:1 mixture of DMF:EtOH affords CP **1** overnight, while a 1:3 mixture leads to CP **2**.

*CP synthesis as single crystals*: a 2:1 mixture of isoquinoline-5-carboxylic acid and $Cu(BF_4)_2$ hexahydrate are dissolved in 10 mL of either a 3:1, or a 1:3 mixture of DMF and EtOH. If after 24 h no crystal had formed, the mixture was left to slowly evaporate at r.t. until the first crystals formed.

Deposition Numbers 2260335 (for CP **1**), 2260336 (for CP **2**), and 2266665 (for [$Co^{II}$(isoquinoline-5-carboxylate)$_2$($H_2O$)$_4$]) contain the supplementary crystallographic data for this paper. These data are provided free of charge by the joint Cambridge Crystallographic Data Centre and Fachinformationszentrum Karlsruhe Access Structures service.

## Conclusions

The exploration of the use of heteroditopic isoquinoline-5-carboxylic acid in the formation of coordination polymers with Cu(II) ions has afforded four different microcrystalline phases (**1**, **1′**, **2** and **3**) depending on the reaction conditions used and the solvent mixture (EtOH : DMF) employed. Two of the above-mentioned materials, CPs **1** and **2**, were also characterized by SC-XRD techniques. They have both a 2D metal ligand connectivity, octahedral Cu(II) ions, each bound to four ligands, but they mainly differ by the role of included solvents. CP **1** has uncoordinated DMF molecules included in linear square shaped channels, while CP **2** displays DMF directly bound to the metal and disordered EtOH within framework unconnected pockets. The different conditions that select CP **1** over CP **2** were explored. Both species can be considered to be kinetic products, with CP **2** relatively more stable than CP **1**, as the latter transforms into the former if the reaction conditions are kept for longer. CP **1** also loses solvent over time if left in ambient conditions, while CP **2** appears to be stable. On the other hand, under refluxing conditions a different phase, **3**, is formed with no solvent included and thus considered to be the thermodynamic product. Although the obtained CPs do not retain porosity upon solvent release and do not show any significant adsorption properties, studies of this type can contribute to understand the various factors which can determine the final structural outcome in coordination polymers made with heteroditopic ligands, identify kinetic *vs.* thermodynamic products, and again demonstrate that small variation in the procedures pertaining the synthesis of coordination polymers can have far than nominal effects.

## Supporting Information Summary

Additional P-XRD plots for CPs **1** and **2** and other phases; additional details on the SC-RXD structures and relative Crystallographic Tables; TGA and BET analysis plots; $CO_2$ adsorption profile for CP **1**.

## *Acknowledgements*

All authors acknowledge Polisocial Award 2020 ( for funding (Project SAFER) and Mr. Andrea Murelli for initial studies on CP **2**. The single crystal x-ray diffraction experiments on [$Co^{II}$-(isoquinoline-5-carboxylate)$_2$($H_2O$)$_4$] were carried out at the Next GAME Laboratory of the Politecnico di Milano, co-funded by Regione Lombardia.

## *Conflict of Interests*

The authors declare no conflict of interest.

## *Data Availability Statement*

The data that support the findings of this study are available from the corresponding author upon reasonable request.

**Keywords:** coordination polymers · heteroditopic ligands · P-XRD · SC-XRD · phase stability

[1] a) S. R. Batten, S. M. Neville, D. R. Turner, in *Coordination Polymers Design, Analysis and Application*, *Stefan Kaskel (Ed.) The Chemistry of Metal-Organic Frameworks Synthesis, Characterization, and Applications*, Wiley-VCH Verlag GmbH & Co. **2016**; b) S. L. James, *Chem. Soc. Rev.* **2003**, *32*, 276; c) M. C. Hong, L. Chen, *Design and Construction of Coordination Polymers*, Wiley, **2009**; d) H. Furukawa, K. E. Cordova, M. O'Keeffe, O. M. Yaghi, *Science* **2013**, *341*, 947; e) M. Lippi, M. Cametti, *Coord. Chem. Rev.* **2021**, *430*, 213661.
[2] a) L. Yu, Z. Wang, J. Wu, S. Tu, K. Ding, *Angew. Chem. Int. Ed.* **2010**, *122*, 3709; b) H. Gildenast, L. Gruszien, F. Friedt, U. Englert, *Dalton Trans.* **2022**, *51*, 7828.
[3] a) N. Yoshinari, T. Konno, *Coord. Chem. Rev.* **2023**, *474*, 214850; b) J. Zhao, J. Yuan, Z. Fang, S. Huang, Z. Chen, F. Qiu, C. Lu, J. Zhu, X. Zhuang, *Coord. Chem. Rev.* **2022**, *471*, 214735; c) A. Y. Robin, K. M. Fromm, *Coord. Chem. Rev.* **2006**, *250*, 2127.
[4] a) F. James Claire, S. M. Tenney, M. M. Li, M. A. Siegler, J. S. Wagner, A. Shoji Hall, T. J. Kempa, *J. Am. Chem. Soc.* **2018**, *140*, 10673; b) J. Conesa-Egea, C. D. Redondo, J. Ignacio Martínez, C. J. Gomez-García, O. Castillo, F. Zamora, P. Amo-Ochoa, *Inorg. Chem.* **2018**, *57*, 7568; c) Y. Miyazaki, Y. Kataoka, W. Mori, T. Kawamoto, *Inorg. Chem. Commun.* **2012**, *25*, 14; d) O. R. Evans, W. Lin, *Chem. Mater.* **2001**, *13*, 3009; Y. Yu, X. Pan, C. Cui, X. Luo, N. Li, H. Mei, Y. Xu, *Inorg. Chem.* **2020**, *59*, 5593; e) L.-Y. Li, G.-X. Duan, J.-Y. Liu, L.-P. Zhang, Y.-P. Xie, X. Lu, *Cryst. Growth Des.* **2020**, *20(6)*, 3795.
[5] J. Y. Lu, A. M. Babb, *Chem. Commun.* **2002**, 1340–1341.
[6] R.-B. Lin, H. Wu, L. Li, X.-L. Tang, Z. Li, J. Gao, H. Cui, W. Zhou, B. Chen, *J. Am. Chem. Soc.* **2018**, *140*, 12940.
[7] a) Z. Chen, S. L. Hanna, L. R. Redfern, D. Alezi, T. Islamoglu, O. K. Farha, *Coord. Chem. Rev.* **2019**, *386*, 32.
[8] a) S. Hu, H.-H. Zou, M.-H. Zeng, Q.-X. Wang, H. Liang, *Cryst. Growth Des.* **2008**, *8*, 2346; b) M. Du, R.-Q. Zou, R.-Q. Zhong, T. Yamada, G. Maruta, S. Takeda, Q. Xu, *Inorg. Chim. Acta* **2008**, *361*, 1827; c) K.-J. Chen, D. G. Madden, T. Pham, K. A. Forrest, A. Kumar, Q.-Y. Yang, W. Xue, B. Space, J. J. Perry, J.-P. Zhang, X.-M. Chen, M. J. Zaworotko, *Angew. Chem. Int. Ed.* **2016**, *55*, 10268; d) X.-H. Bu, M.-L. Tong, Y.-B. Xie, J.-R. Li, H.-C. Chang, S. Kitagawa, J. Ribas, *Inorg. Chem.* **2005**, *44*, 9837.
[9] M. M. Haskins, M. Lusi, M. J. Zaworotko, *Cryst. Growth Des.* **2022**, *22*, 3333.
[10] a) X. Guo, S. Geng, M. Zhuo, Y. Chen, M. J. Zaworotko, P. Cheng, Z. Zhang, *Coord. Chem. Rev.* **2019**, *391*, 44; b) R. Ding, C. Huang, J. Lu, J. Wang, C. Song, J. Wu, H. Hou, Y. Fan, *Inorg. Chem.* **2015**, *54*, 1405.
[11] Calculated with Mercury 2023.2.0, probe radius = 1.2 Å; Approx. grid spacing = 0.7 Å.
[12] H.-C. Yu, L. Li, J. Gao, J. Tong, W. Zheng, M. Cametti, A. Famulari, S. Meille, F. Guo, J. M. Rujas, *Dalton Trans.* **2015**, *44*, 15960.
[13] G. Durgaprasd, D. N. Sathynarayana, C. C. Patel, *Bull. Chem. Soc. Jpn.* **1971**, *44*, 316.

Manuscript received: August 2, 2023